We are IntechOpen,
the world's leading publisher of Open Access books
Built by scientists, for scientists

6,900
Open access books available

185,000
International authors and editors

200M
Downloads

154
Countries delivered to

Our authors are among the

TOP 1%
most cited scientists

12.2%
Contributors from top 500 universities

BOOK CITATION INDEX
CLARIVATE ANALYTICS
INDEXED

WEB OF SCIENCE™

Selection of our books indexed in the Book Citation Index
in Web of Science™ Core Collection (BKCI)

Interested in publishing with us?
Contact book.department@intechopen.com

Numbers displayed above are based on latest data collected.
For more information visit www.intechopen.com

Challenging Evaluation of the Hybrid Technique of Chemical Engineering – Proton NMR Technique for Food Engineering

Yasuyuki Konishi[1,*] and Masayoshi Kobayashi[2]
[1]Hokkaido Industrial Technology Center,
379 Kikyo-cho, Hakodate, Hokkaido
[2]Advanced Technology Institute of Northern Resources,
8-6, Tonden 2-Jo, 2-Chome, Sapporo, Hokkaido
Japan

1. Introduction

In the field of food engineering, chemical engineering and bioengineering have commonly used the data obtained from physicochemical techniques. In particular, water species are strongly related to food quality, as has been demonstrated in the International Symposium on Properties of Water (Eds. Rockland and Stewart, 1981). The water species retained in foods, as is well known, expose their multifunctional nature by dynamically responding to environmental conditions such as temperature, pressure, dehydration processes, water content, etc. For scientific analysis of the multifunctional water species retained in foods, of particular difficulty is the influence of nonlinear dynamic change on food quality. To quantitatively evaluate the nature of the water species, a large number of researchers have demonstrated the diversity of their biological and physicochemical nature using various parameters. The water activity (a_w) has, for example, commonly been used as a parameter to evaluate the deterioration of foods (Fennema, 1976). The effective water diffusivity parameter (*De*) in foods has also frequently been employed to evaluate the dehydration rate (Jason, 1958). From the chemical engineering point of view, this is a typical procedure in evaluating water mobility in the food tissue matrix. Conversely, for direct identification of the water species at the molecular level, magnetic resonance techniques have been applied to evaluate food quality, as demonstrated in the International Conferences on Applications of Magnetic Resonance in Food Science (Eds. Belton *et al.*, 2003).

In our previous papers (Konishi *et al.*, 2001, 2003), using separately chemical engineering and proton NMR techniques, water species retained in fish paste sausage and squid were roughly distinguished into two different species as a function of water content. The two species were water species A_1, to be recognized as the higher water content at $W_0 > 120\%$-d.b. accompanied by higher water diffusivity, *De,* and water species A_2, $W_0 < 120\%$-d.b., with lower *De.* This delineation, however, was unclear because of a vagueness of the boundary

---

[*] Corresponding Author

between the two water species. To clearly discriminate between the two water species, a new technique is needed for the design of food products. In the present study, responding to this need, a hybrid technique derived from joint research using chemical engineering techniques and proton NMR techniques was proposed. The aims of this study are: (1) to demonstrate the dynamism of water species influenced by the change of environmental conditions and the dynamic transformation between the two water species, A_1 and A_2; (2) to quantitatively visualize the limitations of both the chemical engineering technique and the proton NMR technique; (3) to apply a hybrid technique in choosing specified design parameters in order to clearly identify differences between the two water species and among a variety of food products; and (4) to classify twelve commercial jerky products, as a typical example, into a few groups based on the characterization of design parameters using the hybrid technique.

2. Experimental methods of the hybrid technique

2.1 Methods

Six commercially distributed beef and pork jerkies, (BJ-1~BJ-6) and (PJ-1~PJ-6), respectively, a pork meat (designated P_H, used as a reference meat) produced in Hokkaido, two beef meats (B_A: produced in Australia, and B_H: produced in Hokkaido), salmon (SM), and squid (SQ) were chosen as the food samples. All samples used in this study were tabulated in Table 1. The commercial jerkies used were characterized as having a water content range

	Features	Group No.
PJ-1	soy-sauce base taste, about 1.0 mm thick	2
PJ-2	soy-sauce base taste, 1.1~1.4 mm thick	1
PJ-3	light taste, oily, smoked flavor, 0.8~5.9 mm thick	2
PJ-4	salt base taste, smoked flavor, strong taste, hard, 2.2~4.8 mm thick	2
PJ-5	salt base taste, smoked flavor, strong taste, soft, 1.3~2.7 mm thick	3
PJ-6	soy-sauce base taste, light taste, hard, 1.9~3.5 mm thick	3
BJ-1	salt base taste, light taste, hard, 1.4~2.2 mm thick	2
BJ-2	salt base taste, strong taste, soft, about 2.2 mm thick	3
BJ-3	miso-sauce base taste, strong taste, soft, 4.2~5.9 mm thick	3
BJ-4	salt base taste, light taste, soft, 1.6~3.1 mm thick	2
BJ-5	soy-sauce base taste, strong taste, hard, 3.1 mm thick	1
BJ-6	salt base taste, light taste, hard, 0.9~2.8 mm thick	2
P_H	pork meat produced in Hokkaido, soy-sauce base taste, hard, about 6±1.0 mm thick	
B_H	beef meat produced in Hokkaido, about 8±1.0 mm thick	
B_A	beef meat produced in Australia, about 8±1.0 mm thick	
SQ	squid mantle, 50×50×7±1.5 mm	
SM	salmon, 50×15×12~26 mm	

Table 1. Features of the pork meat (P_H), beef meat (B_A and B_H), squid (SQ), salmon (SM), and the commercial jerkies used for this study. PJ-1~-6: pork jerkies; BJ-1~-6: beef jerkies.

of 30~80%-d.b. (dry base, W_D), the pork and beef meats had the initial water contents of 230~320%-d.b. and 230~280%-d.b., respectively, and the initial water content of the salmon and the squid commonly ranged from 300~360%-d.b. To evaluate the effective diffusivity (De) of water species, each of the samples was placed in a stainless steel net tray (4 meshes) that was mechanically hung from a strain gage transducer in the dryer. The sample weight was, to evaluate the dehydration rate, continuously recorded by the output of strain-gage transducer using a data-logger. With molecular-level analysis, to evaluate the correlation time (τ_C) of the water species in the salmon, squid, 12 jerkies, B_H, B_A, and P_H, a nuclear magnetic resonance (NMR) technique was applied to measure the ^{1}H-NMR spectra and the spin-spin relaxation time (T_2) of water protons. All samples, cut into 2×2×10 mm pieces, were inserted into an NMR sample tube (4mm in inner diameter, 180mm in length). ^{1}H-NMR spectra were obtained using a JEOL A-500 FT-NMR spectrometer operating at 500MHz for protons. The observed frequency width was 20 kHz. The 90º pulse width was 12.5 μs, and the number of pulse repetitions was 8. The proton chemical shifts were measured by using a slight amount of water containing deuterium oxide as an external reference. All the NMR measurements were performed at 23.5±0.5ºC. The spin-spin relaxation times, T_2, were obtained by the spin locking method. The hardness (N/m²) of the samples was measured using a creep tester equipped with a V-shaped plunger (30 mm wide, 1 mm thick) to press a 60% of the sample size of 2~8×10×50 mm.

2.2 Evaluation of the parameters

2.2.1 Effective diffusion coefficient (De) of water species

As has been reported by a large number of researchers (Andreu and Stamatopoulos, 1986; Waananen and Okos, 1996; Litchfield and Okos, 1992; Kannan and Bandyopadhyay, 1995), diverse mathematical equations for evaluating the effective diffusion coefficient (De) of water in foods have been demonstrated in various forms. In the present study, De's of all the samples were evaluated by applying Equation (1) to the dehydration response curves obtained. In the present experimental drying conditions, it was reconfirmed that the drying operations were within a falling-rate period. Through all the evaluation of De, the effect of the shrinkage of the samples (derived from the dehydration) on the values obtained was previously evaluated, and the sizes of the samples were corrected.

$$\frac{W - We}{W_D - We} = \left(\frac{8}{\pi^2}\right)^3 exp\left(\frac{-\pi^2 \cdot De \cdot t}{4} \cdot \left(L_a^{-2} + L_b^{-2} + L_c^{-2}\right)\right) \qquad (1)$$

Where W is the water content (%-d.b.) of the sample at $t = t$ (h), We is the equilibrium water content (%-d.b.), W_D is the water content (%-d.b.) at the given initial condition, De is the effective diffusion coefficient (m²/h) of water species retained in the foods, L_a, L_b, and L_c (m) are the half distances of the sample width, and t is dehydration time (h).

De is represented as a function of the structure parameters (porosity and labyrinth factor) of food and the activation energy, as shown in Equation (2).

$$De = \left(\frac{\varepsilon}{\chi}\right) \cdot D = \delta \cdot D_0 \cdot exp\left[\frac{-E_D}{R \cdot (T_D + 273)}\right] \qquad (2)$$

Where ε is porosity, χ is labyrinth factor, D is diffusivity (m²/h), D_0 is the frequency factor of D, δ is diffusibility (= ε/χ), E_D is activation energy of De, R is gas constant, and T_D is drying temperature.

The pre-exponential factor, $\delta \cdot D_0$, can be a useful tool to discriminate between the water species retained in different kinds of foods, as is described in upcoming sections.

2.2.2 Correlation time (τ_C) of water protons

The spin-locking pulse technique used was effective in detecting a very fast relaxation signal at low water contents. For evaluation of the relaxation time, T_2, the equation $M_t = M_0\, exp(-ts/T_2)$ was used, where M_t is the magnitude of the magnetization vector after the spin locking pulse, M_0 is magnitude of the macroscopic equilibrium magnetization vector, and ts is the spin locking pulse length. In the present study, the plot of $ln\,[M_t\,/\,M_0]$ vs. ts indicated good linearity (which demonstrates a correlation coefficient higher than 0.99) through all water content of the foods, suggesting that the evaluated T_2 value was reasonable. From T_2, the correlation time of a water proton, τ_C, was evaluated using Equation (3) as described by Abragam (1963):

$$\frac{1}{T_2} = \frac{\gamma^4 \cdot \hbar^2 \cdot I(I+1)}{5r^6}\left(3\tau_c + \frac{5\tau_c}{1+\omega_0^2 \cdot \tau_c^2} + \frac{2\tau_c}{1+4\omega_0^2 \cdot \tau_c^2}\right) \quad , \qquad (3)$$

where γ is the gyromagnetic ratio of a proton (= 2.675×10^8 rad·T⁻¹·s⁻¹), $\hbar$ is the modified Plank's constant (6.63×10^{-34} J·s), I is the nuclear-spin quantum number of a water proton (= 0.5), r is the proton-proton distance of a water molecule (0.16 nm), ω_0 is the resonance frequency of NMR (= 3.14×10^9 s⁻¹), and τ_C is the correlation time of a water proton (s).

3. Dynamic transformation of water species retained in foods

3.1 Variety of water species in foods

3.1.1 Visualization from the proton NMR technique

The water species retained in foods are dynamically changed into multifunctional states according to environmental conditions such as temperature, atmospheric pressure, atmospheric relative humidity, seasoning components such as salt and sugar, concentration of seasoning components, etc. Figure 1 is a schematic explanation of the water species adsorbed on macromolecules such as proteins in foods. The water species are classified into three groups as: (1) monolayer adsorbed water localized in region-I, which is referred to as bond water, immobilized water, or non-freezing water; (2) multi-adsorbed water localized in region-II, which is referred to as strongly restricted water, glass-state water, etc.; and (3) free water localized in region-III, which is referred to as normal isotropic bulk water, capillary condensation water, etc. The proton NMR technique produced correlation times of the three regions, I, II, and III, as τ_C = $10^{-6\sim-7}$s, $10^{-6\sim-11}$s, and 10^{-12}s, respectively. This classification is interestingly correlated to the three regions of the adsorption isotherm evaluated by the chemical engineering technique, as shown in Figure 2 by curve 1. As has been reported in previous papers (Konishi et al., 2003, 2010), water species in the three regions are dynamically transformed by each other depending on environmental conditions in
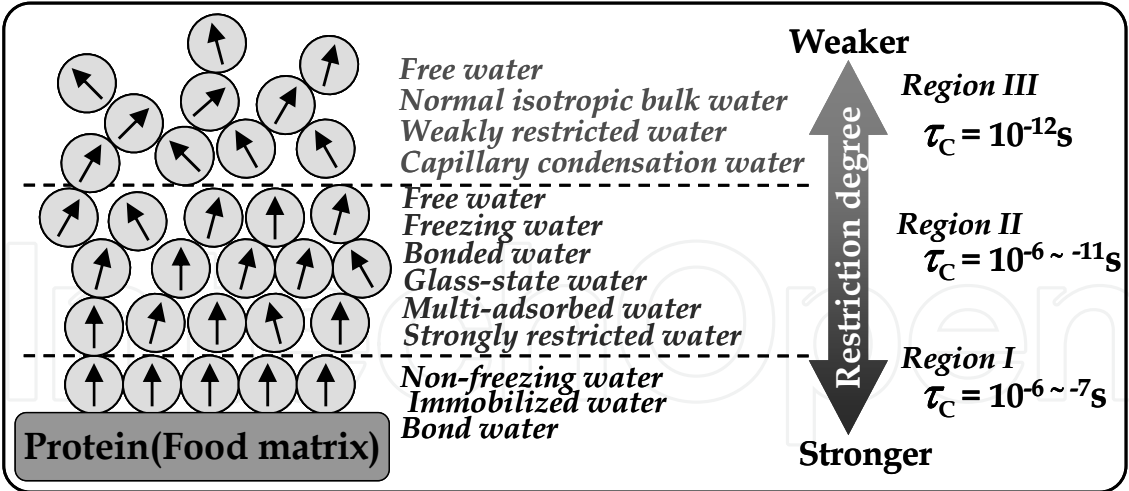
Fig. 1. Schematic explanation of the water species adsorbed on macromolecules in food.
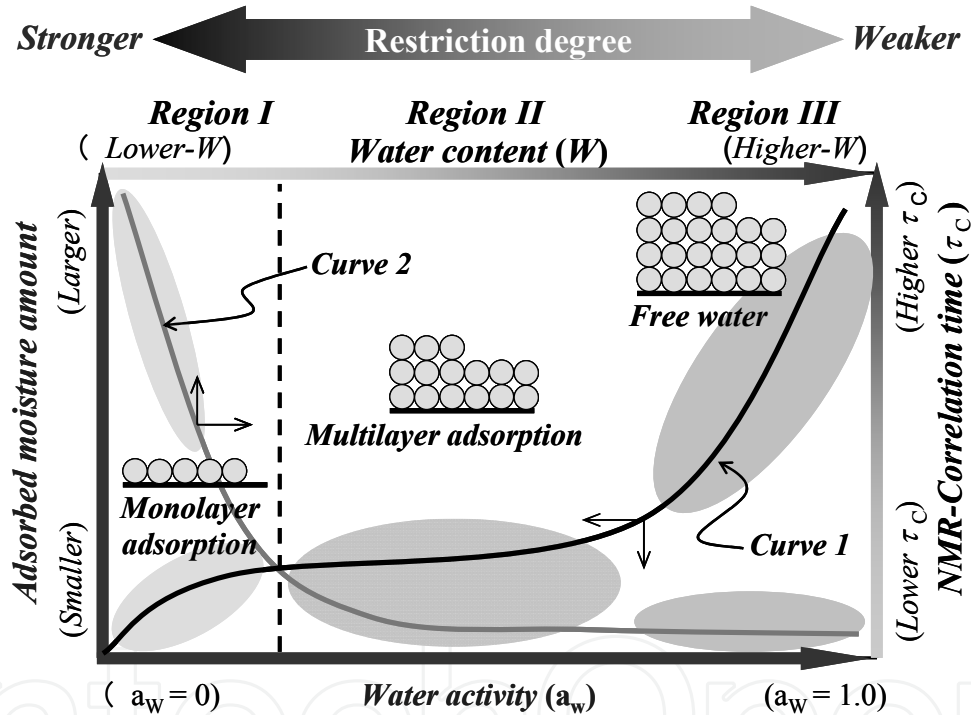

Fig. 2. Classification of the adsorbed water species in the food tissue matrix.

conjunction with the progress of dehydration. In atmospheric conditions, according to the progress of dehydration, the free water species in region III is preferentially removed rather than the two water species in regions I and II.

3.1.2 Visualization from the chemical engineering technique

Taking into account the water activity map presented by Labuza *et al.* (1970) and Schmidt (2004), one may visualize three regions on a water activity space. Fig. 2 shows a schematic explanation of the specified two curves: curve 1 for the water adsorption isotherm of food systems as a function of water activity (the isotherm was divided again into three regions, I, II, and III) and curve 2 for the NMR correlation time (τ_C) of water species retained in food as

a function of water content (W_0). As can be seen from the comparison of the two curves, the water species adsorbed in region I with lower water activity contributes to the higher correlation time (τ_C). The higher τ_C means higher restriction strength derived from the food tissues. The water species adsorbed in the region III with higher water activity, contributing to lower τ_C, which means lower restriction strength. These results bring about an inverse relation between the two parameters, τ_C (curve 2), and the adsorbed water amount (curve 1) as shown in Fig. 2. This relation can be usefully employed in the hybrid technique as is described in upcoming sections.

The three water species distributed in regions I, II, and III presented in Figs. 1 and 2 can be further classified as species A_1 and species A_2. The water species in regions I and III belong to species A_2 and species A_1, respectively. The water species in region II belongs to an intermediate species between species A_1 and species A_2. Figure 3 schematically illustrates the water species A_1 and A_2 retained in foods as a model description. From the schematic visualization, one may recognize water species A_1 to be weakly restricted by macromolecules in foods, such as proteins, at greater water content and water species A_2 to be strongly restricted due to the progress of dehydration. The space formed due to the dehydration in region III in Fig. 1 would create micropores resulting in higher porosity (ε) and higher labyrinth factor (χ) in the food tissue matrix. These micropores would be filled again with water species when re-hydration occurred, indicating a reproducibility of the adsorbed water species as is discussed in upcoming sections (see Fig. 5).
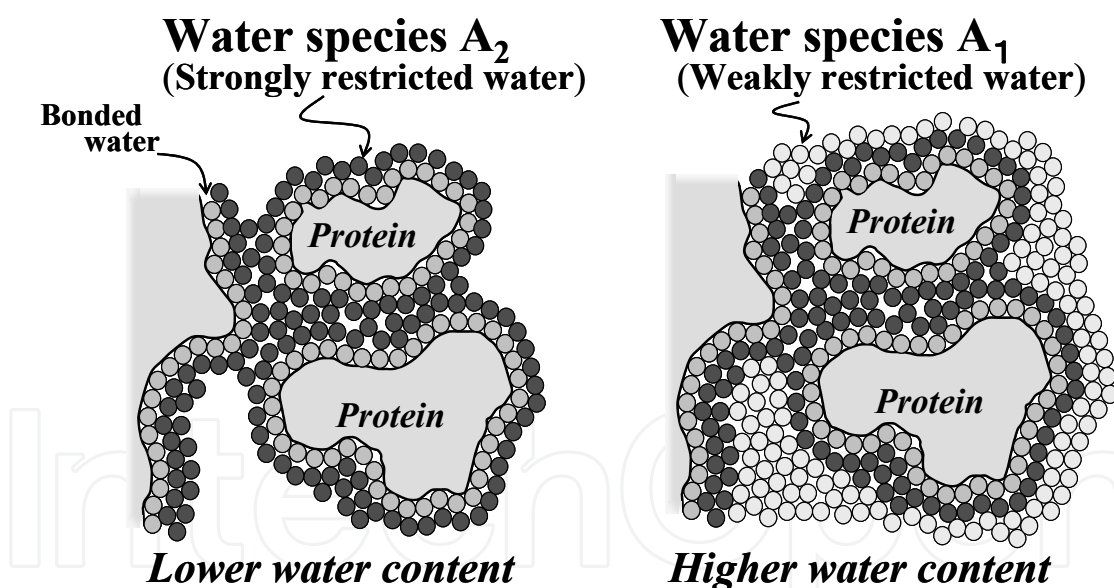

Fig. 3. Schematic explanations of the adsorbed states for water species in foods.

3.2 Dynamism and reversibility of the water species in foods identified by the proton NMR technique

The proton NMR spectrum clearly demonstrates the dynamism of water species derived from the dehydration of the sample (Konishi *et al.*, 2010). Figure 4 demonstrates the dynamism of the reduced amount of water species (the dehydration of squid) as a steep reduction of the proton NMR spectra of peak-A. The three peeks, A, B, and C, were identified in our previous work (Konishi *et al.*, 2010) as weakly restricted water, strongly
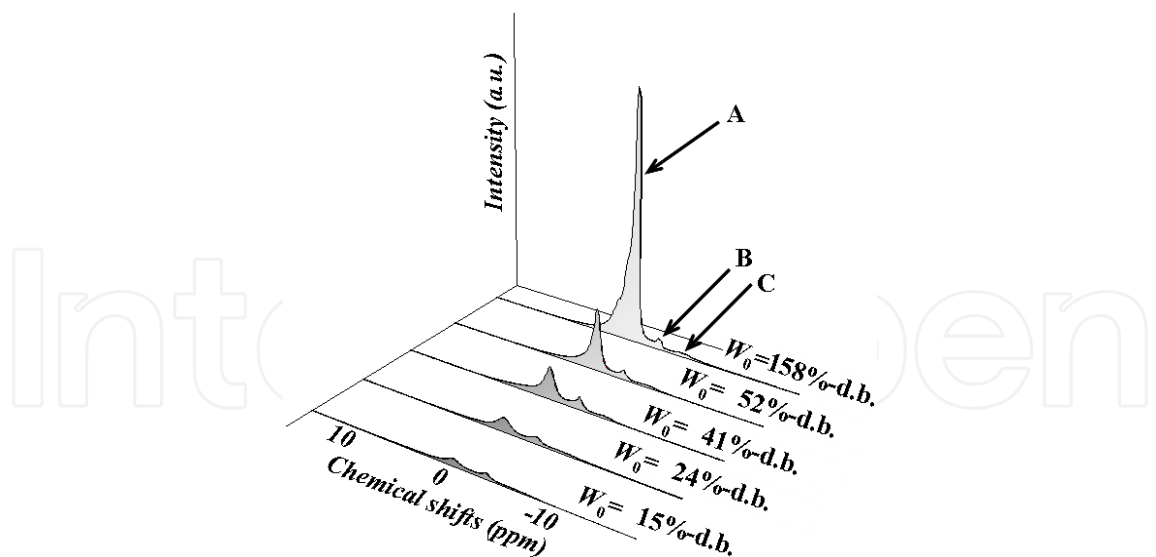
Fig. 4. Dynamic behavior of ^{1}H-NMR spectra for species A, B, and C in the squid muscle in the course of a drying operation.

restricted water, and lipids, respectively. One may recognize the reduction of only peak-A due to dehydration, whereas peaks-B and -C gave an identical value indicating that the two species are not influenced by dehydration.

Focusing on the reversibility of peak-A, one can easily recognize the dynamism of proton NMR spectra of water species in the squid, as shown in Figure 5. The strength of peak-A was steeply reduced by dehydration (see curve (1)), and the peak height was restored by re-hydration (see curve (2)), whereas the peaks-B and -C kept the same peak height regardless of dehydration and re-hydration. This reproducibility of peak-A strongly demonstrates the ability
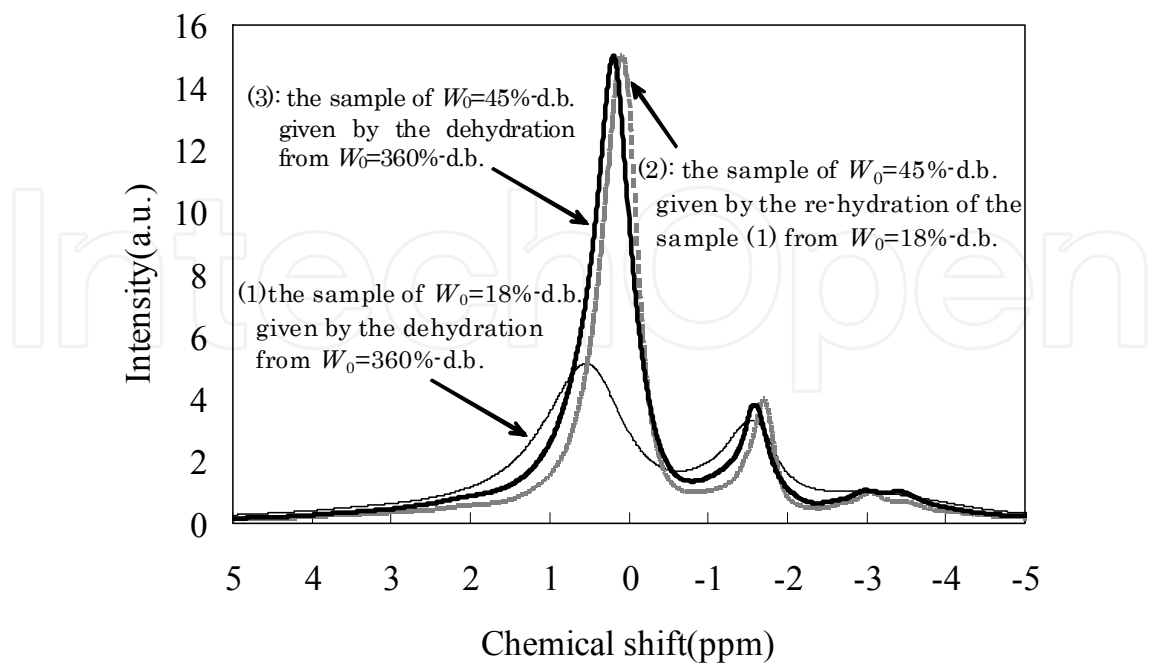
Fig. 5. Reproduced dynamic behavior of ^{1}H-NMR spectra for species-A, -B and -C in the squid muscle.

of water species A_1 and A_2 to be reformed in the food tissue matrix through re- hydration. This reversibility is a very important factor for dried food products because, generally speaking, dried foods are frequently re-hydrated before being consumed (dried kelp, dried green onions, and dried noodles, etc.). Exploitation of reversible water species in dried foods could produce the same taste as when the food is freshly prepared. To evaluate the reproducibility of dried food taste, one should focus on τ_C because the τ_C value is closely related to the concentration of seasoning and the kind of food. The reproducibility of τ_C is, therefore, an important factor for taste reproducibility. Figure 6 demonstrates the reproducibility of τ_C as a function of W_0. The results show positive reproducibility of τ_C, indicating favorable taste reproducibility in the case of dried squid.
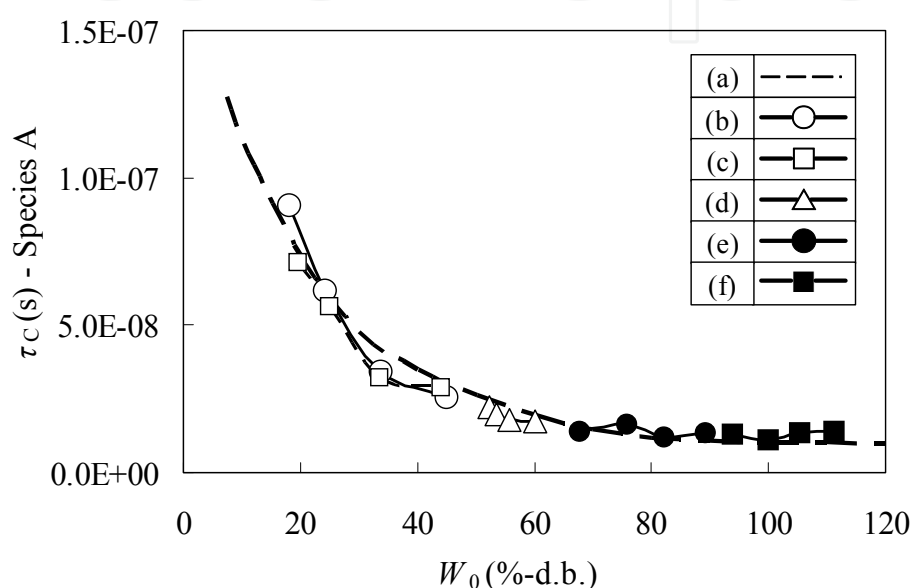
Fig. 6. Reproducibility of τ_C(species A) observed between the dehydration and the water-readsorption operations for the squid muscle: (a) under the continuous drying operation from $W_0 = 120\%$-d.b. to 10%-d.b., (b) after the gradual readsorption of water from $W_0 = 18\%$-d.b. to $W_0 = 45\%$-d.b., (c) from $W_0 = 20\%$-d.b. to $W_0 = 44\%$-d.b., (d) from $W_0 = 50\%$-d.b. to $W_0 = 60\%$-d.b., (e) from $W_0 = 68\%$-d.b. to $W_0 = 89\%$-d.b., and (f) from $W_0 = 94\%$-d.b. to $W_0 = 111\%$-d.b.

4. Limitations of the proton NMR technique

To design the food products requested by the markets, the design parameters chosen should be able to clearly discriminate between various kinds of foods depending on requirements. In particular, the water species retained in the foods should be characterized by the kinds of foods and environmental influences such as temperature, atmospheric pressure, water content, etc. Although the proton NMR water species evaluation technique is a useful tool, one should recognize that the method has some difficulty discriminating among water species retained in foods. Figure 7 illustrates the τ_C values as a function of W_0 for B_A, B_H, and P_H. The $\tau_C \sim W_0$ curves obtained could not discriminate among the three meats, B_A, B_H, and P_H (Konishi and Kobayashi, 2009), even though the water species A_1 and A_2 are roughly distinguished at the critical point of $\tau_C = C\tau_C = 10^{-8}$ s. This unclear discrimination between the three curves can be understood as a limitation of the proton NMR technique.
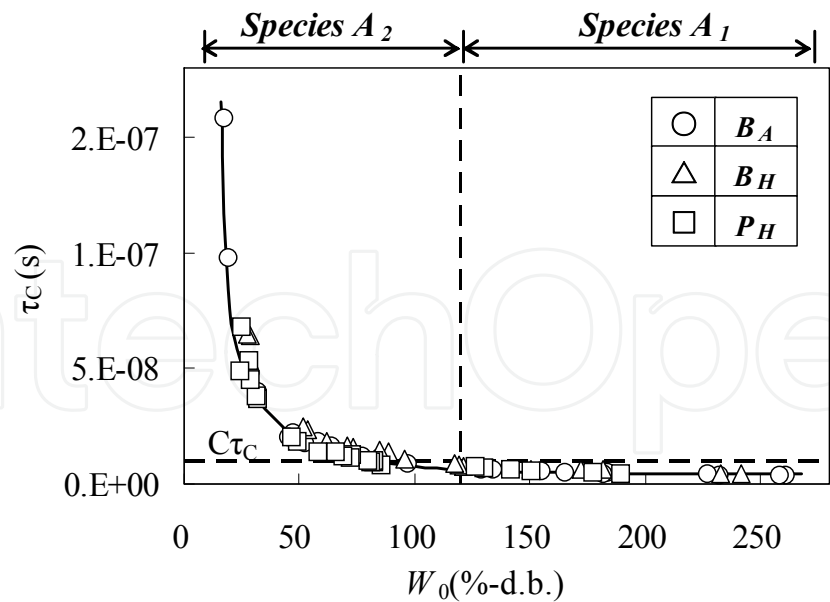
Fig. 7. τ_C as a function of W_0 for B_A, B_H, and P_H.

Figure 8 illustrates τ_C as a function of water content (W_0) of the 12 jerkies and the P_H. The solid line for P_H indicated a steep increase with decreasing W_0, between the values of τ_C = 1.0×10^{-8}s and τ_C = 1.1×10^{-7}s. Since τ_C indicates rotation time of the water species, the steep increase of τ_C demonstrates that the restriction strength of the water species in this region increases markedly upon dehydration from W_0 = 120 to 20%-d.b. Similar results were also obtained for the beef (Konishi and Kobayashi, 2009). The τ_C for the jerkies, on the other hand, fell around the solid line of P_H. From these results, one can recognize that it is difficult to distinguish among the three τ_C –W_0 curves for the pork jerkies, beef jerkies, and P_H, indicating again a limitation of the proton NMR technique.
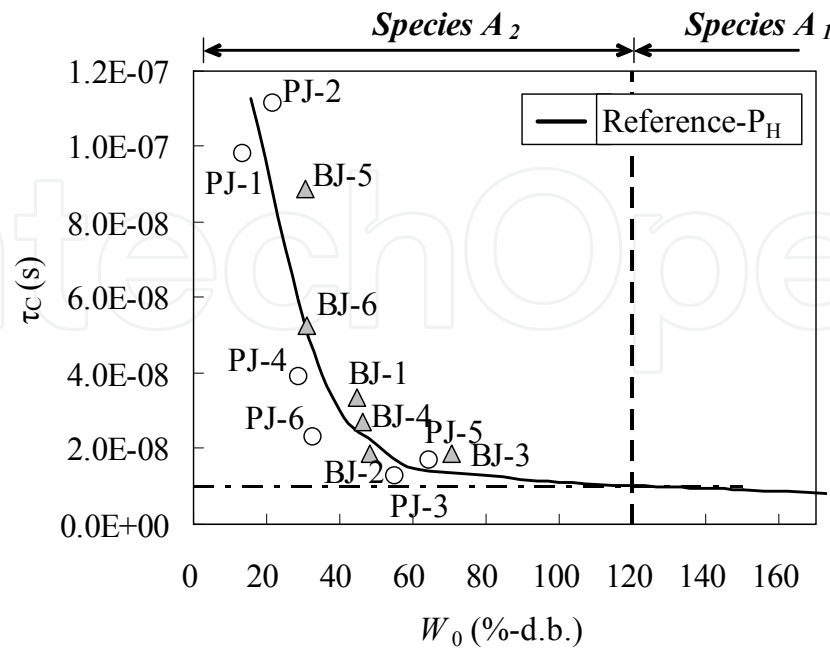

Fig. 8. τ_C as a function of W_0 for the pork and beef jerkies (open circle and closed triangle) and the pork (solid line).

5. Limitation of the chemical engineering technique

5.1 Unclear discrimination of water activity in foods in the chemical engineering technique

Water activity (a_w) has conveniently been used to design food products because of the ease of evaluating the variable using the chemical engineering technique (Fennema, 1976). Figure 9 illustrates a_w as a function of W_0 for the squid and the salmon. As can be seen from the comparison between the two curves, an identical curve was obtained without detecting any difference between the squid and the salmon. This result strongly indicates a limitation of the chemical engineering technique. To develop a new food product, one should choose another parameter for discriminating among products. To address this issue, a computer simulation method for developing new food design parameters is proposed in the next section.
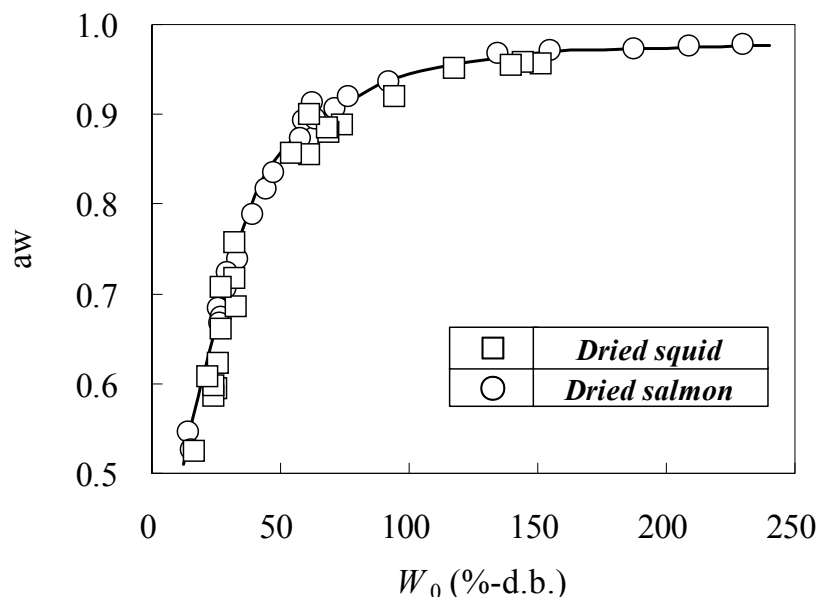
Fig. 9. a_w as a function of W_0 for the salmon and squid.

5.2 Ambiguous physical meaning of the chemical engineering parameters derived from a computer simulation for the dehydration dynamism of salmon

5.2.1 Dehydration dynamism of the water species in the salmon

To characterize the water species retained in the salmon, dehydration response curves could effectively be employed. Figure 10 illustrates the dehydration response curves as a function of the water content of the salmon. The five samples of $W_0 = 54$, 99, 144, 200, and 252%-d.b. were prepared from a sample of $W_0 = 342$%-d.b., and each of the samples was treated by a PUP-operation (poultice up: the samples were stored in a dark room at $T = 2^oC$ for 24 h before use; this operation was conducted to provide homogeneity of water distribution in the sample). The PUP operation contributes to the stepwise increase of the dehydration rate, as shown in Figure 11, by the curves of $b' \sim f'$. Focusing on the five points of $b \sim f$ on the dehydration curve of $W_0 = 342$%-d.b. in Fig. 11(A), the dehydration rates of the five samples clearly demonstrate a stepwise increase, as shown in Fig. 11(B), by the curves of $b' \sim f'$ due to PUP operation. One can recognize that curves $b' \sim f'$ demonstrate a monotonous decay
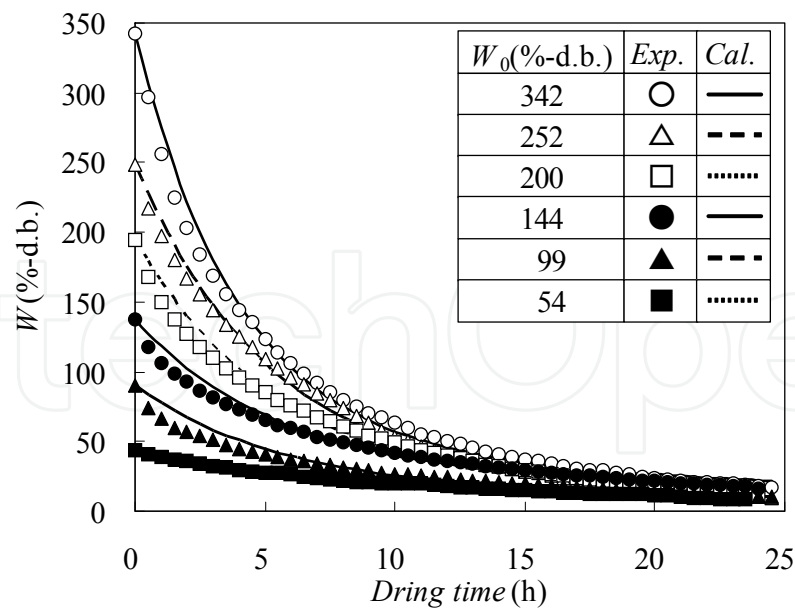
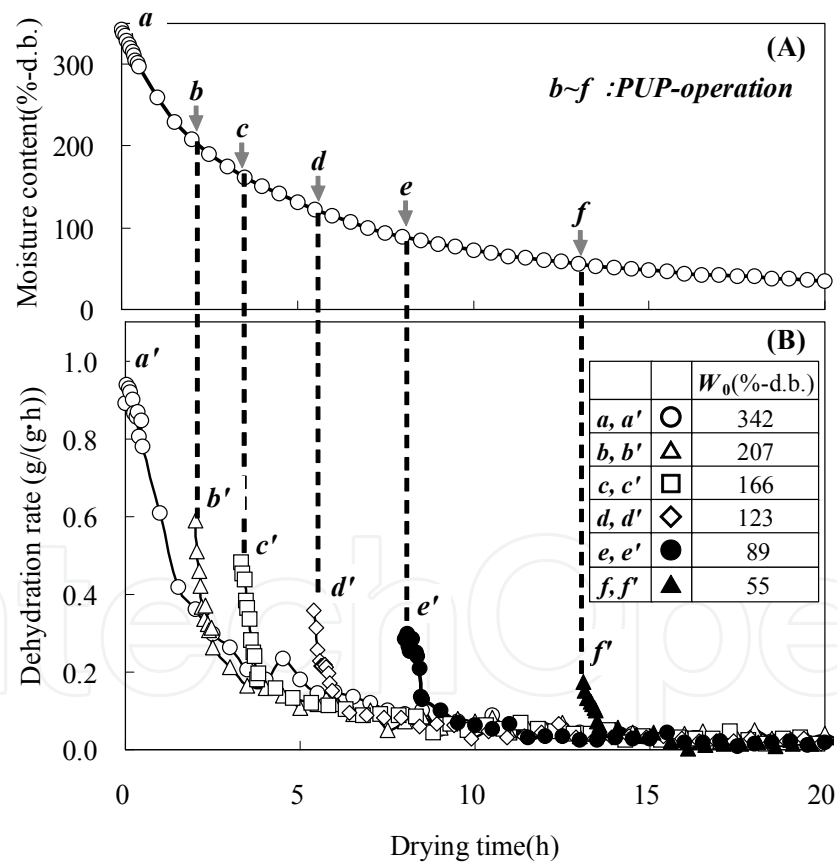Fig. 10. Dehydration response curves of the salmon (T_D = 45°C).

Fig. 11. Acceleration behavior of dehydration rate derived from the PUP operation for the salmon (T_D = 45°C).

curve reaching finally to the curve of a' with an increase in the elapsed time. Using the dehydration rates obtained, the effective diffusivity of the water species, De, can be evaluated as a function of W_0 by applying Equation (1).

5.2.2 Physicochemical mobility (*De*) of the water species

One can recognize the *De* value as a physicochemical mobility of the water species retained in the foods. Figure 12 illustrates *De* for the salmon as a function of W_0 and temperature. Although the data are widely scattered, one can roughly recognize two different water species (species A_1 and A_2) formed in the salmon, depending on the values of W_0. The two water species were divided at about $W_0 = 120\%$-d.b., indicating an identical *De* for the water species A_1 region between $W_0 = 120$ and 360%-d.b. and a gradual decrease of *De* for the water species A_2 region with decreasing W_0 at 35~55°C. Using a rough evaluation of *De* obtained at the three temperatures, one would roughly construct the Arrhenius plots as shown in Figure 13. The slopes of the straight lines seem to give different activation energies depending on the water content of the samples.
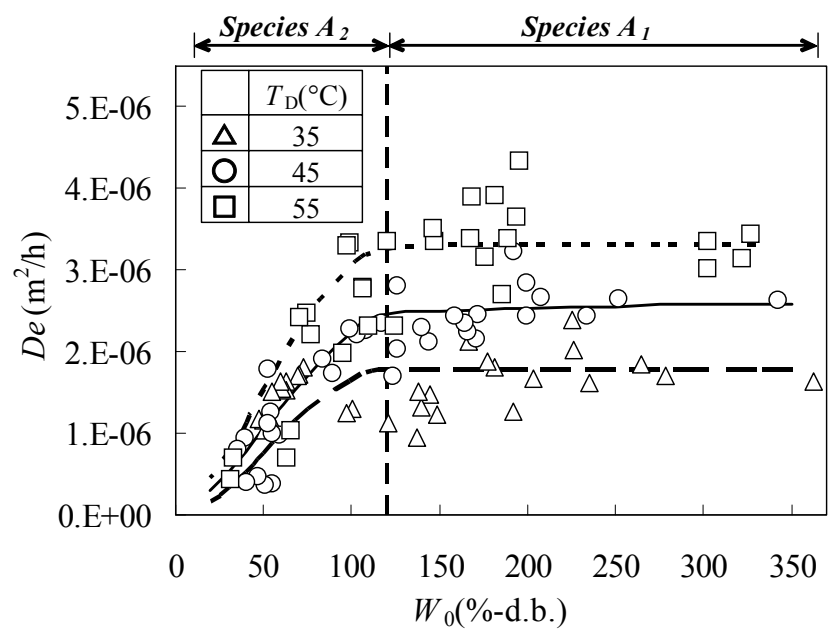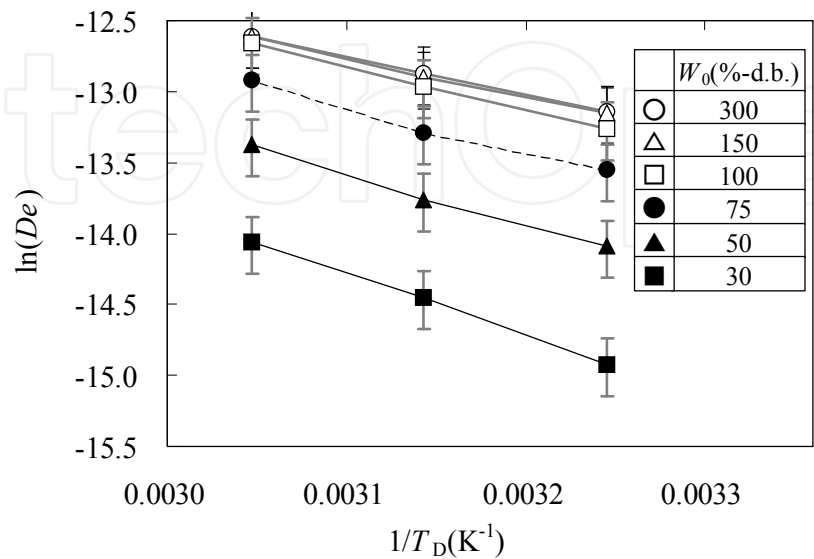

Fig. 12. *De* as a function of W_0 in the salmon.

Fig. 13. Arrhenius plots of *De* for the salmon.

Figure 14 demonstrates E_D as a function of W_0. The activation energy obtained, the E_D values, demonstrates again two water species, A_1 and A_2, divided at $W_0 = 120\%$-d.b. E_D in the water species A_1 region gave an identical value of 22 (±4) kJ/mol and a gradual increase from 20 to 38 (±8)kJ/mol with decreasing W_0. Taking into account the restriction of water species growth that accompanies increased dehydration, one can observe evidence of the activation energy growth (indicating a difficulty of the molecular diffusion of water species in the food tissue matrix due to the growth of the restriction strength) as a result of the decrease of water species mobility (*De*).
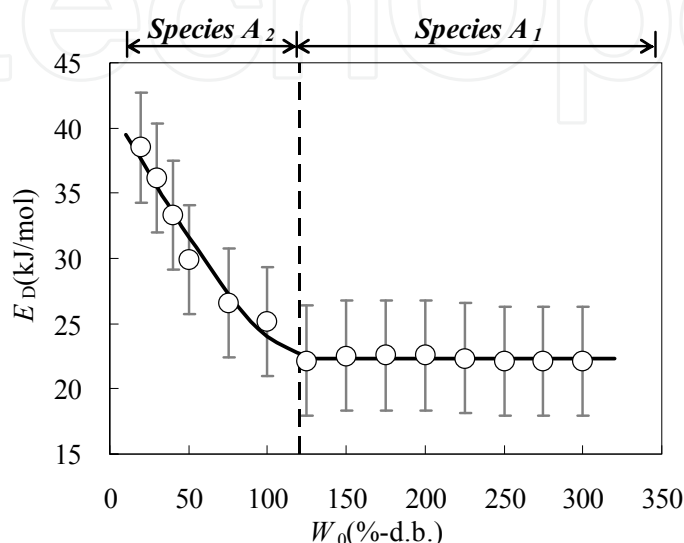

Fig. 14. E_D as a function of W_0 for the salmon.

As for a reason that the activation energy was drastically changed at $W_0 = 120$ %-d.b., it can be attributed to a change in the physical structure of the food tissue matrix due to progressive dehydration. The value of $W_0 = 120\%$-d.b. corresponds exactly to the critical value of τ_C ($C\tau_C = 10^{-8}$s), at which water species A_1 and A_2 were divided according to their restriction strength, and the pre-exponential factor (PF = $\delta \cdot D_0$) of *De* showed steep growth with decreasing W_0 (as will be discussed in the upcoming section, see Fig. 16). The steep growth of PF resulted from the drastic change in the porosity and labyrinth factor of the salmon at $W_0 = 120$ %-d.b. accompanied by the gradual reduction of *De* decreasing W_0.

5.2.3 Water tank model for the computer simulation of the dehydration response curves

The transient response curves of dehydration in the drying operation of foods have been simulated using various mathematical models (Chhinnan, 1984; Madamba *et al.*, 1996; Thompson *et al.*, 1968; Noomhorm and Verma, 1986). In the present study, the dehydration response curves of the salmon presented in Fig. 10 are simulated using a water tank model as a first approximation. The water species retained in the sample are portioned to two different water tanks and the two tanks are respectively filled by the two different water species, A_1 (weakly restricted water species) and A_2 (strongly restricted water species), as shown in Figure 15 (Konishi *et al.*, 2001). During the drying operation, the two water species in the tanks are simultaneously drained by regulating the two valves as mass transfer coefficient, k_W (h^{-1}) and k_S (h^{-1}).
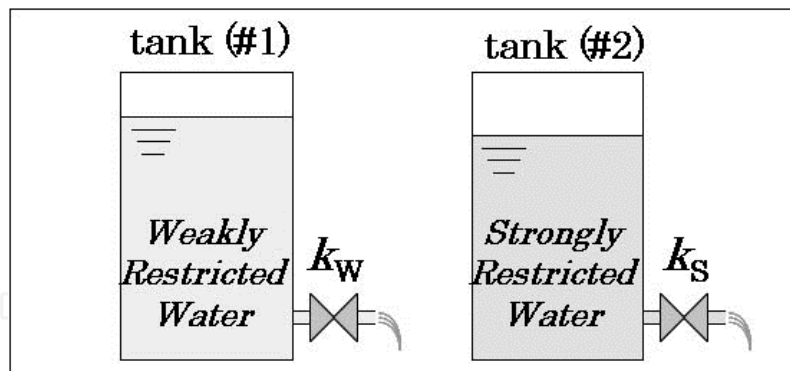
Fig. 15. Schematic explanation of the water tank model proposed as a dehydration of food.

On the material balance equation in the course of the dehydration operation presented in Fig. 10, the water content (W), presented as a perpendicular axis of Fig. 10, can be replaced by the water ratio, $W_R = (W\text{-}We)/(W_D\text{-}We)$, where We is the equilibrium water content (%-d.b.) and W_D is the initial water content of the sample. The dynamism of W_R for the two tanks is expressed by Equation (4).

$$\left(-\frac{dW_{RI}}{dt}\right) = \left(-\frac{dW_{Rw}}{dt}\right) + \left(-\frac{dW_{Rs}}{dt}\right) \tag{4}$$

$$-\frac{dW_{Rw}}{dt} = k_w \cdot W_{Rw} \tag{5}$$

$$-\frac{dW_{Rs}}{dt} = k_s \cdot W_{Rs} \ , \tag{6}$$

where W_{RW} is the ratio of the weakly restricted water species ($=(W_W\text{-}We)/(W\text{-}W_D)$), W_{RS} is the ratio of the strongly restricted water species ($=(W_S\text{-}We)/(W\text{-}W_D)$), W_W is the amount of weakly restricted water species (%-d.b.), and W_S is the amount of strongly restricted water species (%-d.b.).

The differential equation (4) is easily solved and expressed by Equation (7).

$$W_R = \frac{W - We}{W_D - We} = W_{R1} \exp\left[k_s \exp\left(\frac{-E_D}{R \cdot (T_D + 273)}\right) \cdot t\right]$$
$$+ W_{R2} \exp\left[k_w \exp\left(\frac{-E_D}{R \cdot (T_D + 273)}\right) \cdot t\right] \tag{7}$$

$$k_s = \beta_1 \cdot De^0 \tag{8}$$

$$k_w = \beta_2 \cdot De^0 \ , \tag{9}$$

where W_{R1} and W_{R2} are a proportion of the strongly restricted water amount and the weakly restricted water amount, respectively, and k_S (h^{-1}) and k_W (h^{-1}) are the mass transfer coefficient of the strongly restricted water species and of the weakly restricted water species,

respectively. De^0 (= $\delta \cdot D_0$) is the pre-exponential factor of De, and β_1 and β_2 are the constants evaluated by a curve fitting simulation between the experimental and the calculated curves as shown in Fig. 10. The curve fitting obtained showed favorable agreement with the experimental dehydration curves as shown in Fig. 10 by solid curves.

5.2.4 Discrimination of water species A_1 and A_2 due to the pre-exponential factor (De^0) of De

The pre-exponential factor, De^0, can easily be evaluated by the extrapolation of the Arrhenius plot lines against the perpendicular axes in Fig. 13. Figure 16(A) illustrates De^0 as a function of W. The De^0 values obtained were of identical value regardless of W in the water species A_1 region, whereas in the water species A_2 region, there was a steep increase with decreasing W_0.
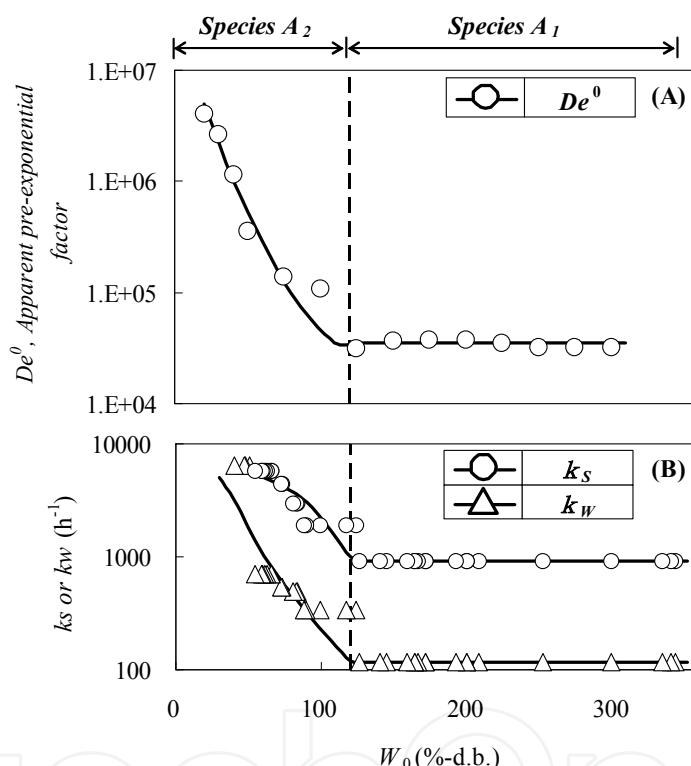

Fig. 16. Pre-exponential factor (De^0) and the dehydration parameters for the computer simulation (k_S, k_W) as a function of W_0 (T_D = 45°C) for the salmon.

Figure 16(B) illustrates k_S and k_W as a function of W_0. The two values show tendencies similar to De^0 even though they can be evaluated by the computer simulation. Comparing the two values between k_S (or k_W) and De^0, one can generate a linear relation between the two values as shown in Figure 17. The parameters of k_S and k_W roughly demonstrate the equations of k_S = 0.025(±0.008) De^0 and k_W = 0.007(±0.004) De^0. Using Equations (8) and (9), one may evaluate β_1 = 0.025(±0.008) and β_2 = 0.007(±0.004). Concerning the physical meaning of β_1 and β_2, since the two parameters were evaluated by the computer fitting simulation, they seem to be meaningless. This evidence indicates a disadvantage of the chemical engineering technique, even though the linear relation between k_S (or k_W) and De^0 would cause the presumption of a relationship between the two parameters.
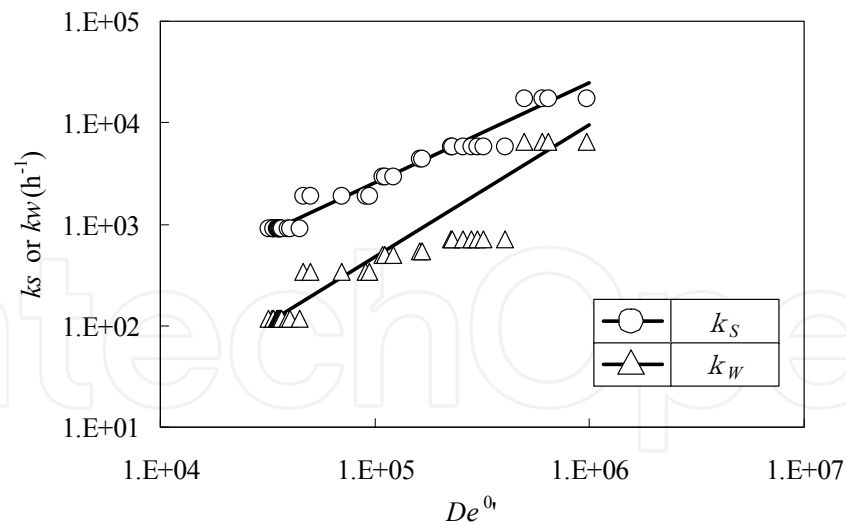
Fig. 17. Dehydration parameters (ks and kw) as a function of pre-exponential factor (De^0)(T_D=45°C) for the salmon.

6. Advantages derived from the hybrid technique

6.1 Visualized correlation between molecular mobility (τ_C) and physicochemical mobility (*De*)

Physicochemical mobility, *De*, which is evaluated by the chemical engineering technique (Fig. 12), and molecular mobility, τ_C, which is evaluated by the proton NMR technique (Fig. 8), are important parameters for characterizing the water species retained in foods as the diffusion rate in the three dimensional space of the food tissue matrix and as the rotation time of water molecules, respectively. The two parameters (*De* and τ_C) for the pork meat (P_H) and 12 jerkies are interestingly related, as shown in Figure 18. This clearly shows an advantage of the hybrid technique. *De* for P_H demonstrates a drastic change at $\tau_C = 10^{-8}$ s,
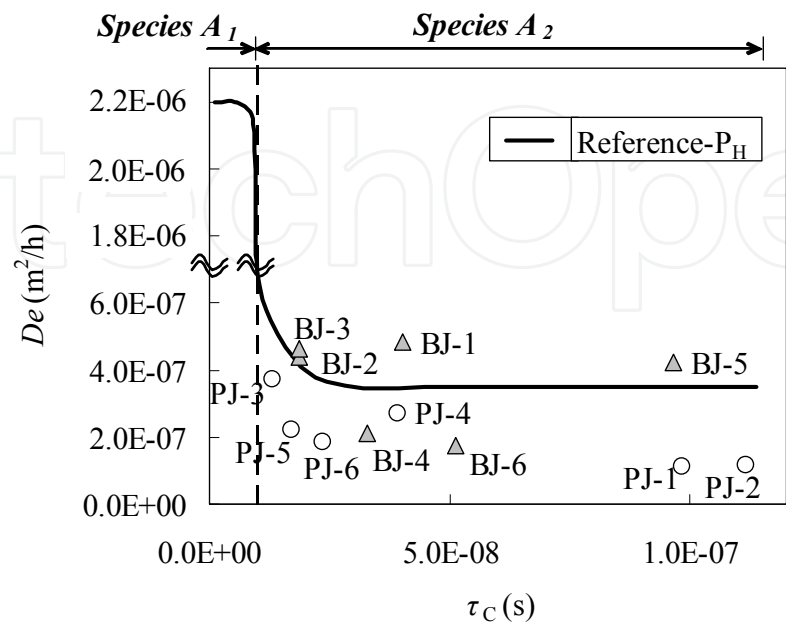

Fig. 18. *De* as a function of τ_C for jerkies and P_H.

indicating an identical De = 2.2(±0.2)×10⁻⁶ m²/h in the species A_1 region and De = 3.5(±1.0) ×10⁻⁷ m²/h in the water species A_2 region. All the De values for the commercial jerkies are distributed in the water species A_2 region, indicating an identical De = 3.0(±1.8)×10⁻⁷ m²/h, which, even though the data are widely scattered, is the same as P_H. Regarding the jerky data, although all the samples distributed in the market commonly use the water species A_2 not A_1 and the effective diffusivity, De, falling in the range of 1.0~5.0×10⁻⁷ m²/h, τ_C is widely distributed in the range of 10⁻⁸ ~ 1.1×10⁻⁷ s. Since each of the jerkies used in this study has own taste different from other, the wide distribution of τ_C has an important meaning in developing different tastes in jerky. This idea is also supported in an upcoming section.

6.2 Clear discrimination of the two water species due to diffusivity (De)

As has been demonstrated in Fig. 12, the De~W_0 plots could not clearly discriminate the water species A_1 and A_2. The De~τ_C plots derived from the hybrid technique, on the other hand, are conveniently able to visualize the discrimination between beef and pork and the two water species, A_1 and A_2, as shown in Figure 19. In particular, the boundary of the two water species is clearly recognized as $C\tau_C$ =10⁻⁸ s, indicating an advantage of the hybrid technique. Focusing on the behavior of B_A, B_H, and P_H, the De values gave a constant value in the two water species regions: in the A_1 region, as 3.1(±0.5) ×10⁻⁶, 4.7(±0.1) ×10⁻⁶, and 2.2(±0.3) ×10⁻⁶ m²/h, respectively; in the A_2 region, as 1.8(±0.5) ×10⁻⁶, 2.0(±0.4) ×10⁻⁶, and 7.0(±1.0) ×10⁻⁷ m²/h, respectively, even though τ_C is significantly changed from 10⁻⁸ to 4.5×10⁻⁸ s. These results suggest the water species A_2 has the interesting characteristic of being able to make a wide shift of the molecular mobility, τ_C, without changing in the De values. This result indicates that, by changing the value of τ_C as a design parameter for food products, the character of various meats can be significantly altered. The hardness of various meats and salmon, for example, can also be controlled by a change in τ_C, as shown in the next section.
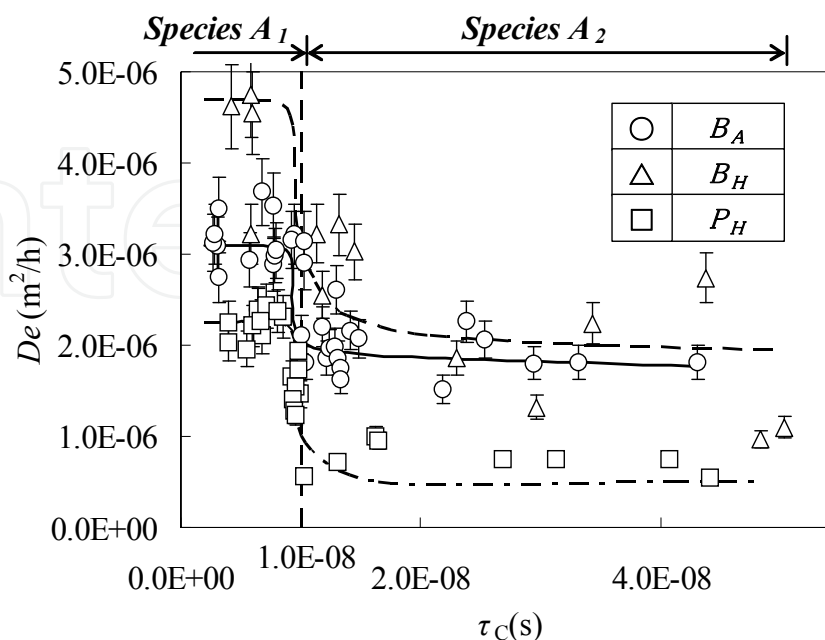

Fig. 19. Comparing behavior of De among B_A, B_H, and P_H as a function of τ_C at 70°C.

6.3 Clear discrimination of the two water species by hardness

Figure 20 demonstrates the hardness of B_A, B_H, P_H, and salmon as a function of τ_C. The hardness of all the samples shows a drastic increase at $C\tau_C = 10^{-8}$ s with increasing τ_C in the water species A_2 region. This clear discrimination between the water species A_1 and A_2 is an advantage of the hybrid technique. One may recognize that the N_P value in the water species A_1 region commonly showed $1.0(\pm 0.5) \times 10^6$ N/m^2 regardless of τ_C in all the samples, whereas in the water species A_2 region and at the range of $\tau_C = 3\times10^{-8} \sim 6\times10^{-8}$ s, it varied widely depending on the samples, as with $N_P = 1.5\times10^7$ for B_A, 1.3×10^7 for B_H, and 1×10^7 N/m^2 for P_H at $\tau_C = 5.0\times10^{-8}$ s. From these results, one can recognize that it is possible to design food products with different N_P values without changing the τ_C values, and it's possible to design products with different τ_C values without changing the N_P values. Keeping $N_P = 1.0\times10^7$ N/m^2, for example, one can have different τ_C values such as $\tau_C = 2.9\times10^{-8}$ s for B_A, $\tau_C = 3.5\times10^{-8}$ s for B_H, and $\tau_C = 4.8\times10^{-8}$ s for P_H. Although the physical meaning of this τ_C value shift is still unclear, it can be attributed to the taste difference between B_A, B_H, and P_H because concrete evidence that the τ_C value changes depending on the kind of food, the concentration of seasonings, and the kind of seasonings has been obtained. Details of these results will be reported in an upcoming work (Konishi and Kobayashi, 2011).

The visualization of $N_P \sim \tau_C$ exhibited in Fig. 20 clearly demonstrates the hybrid technique as a useful tool for discriminating between the two water species and among the kinds of food.
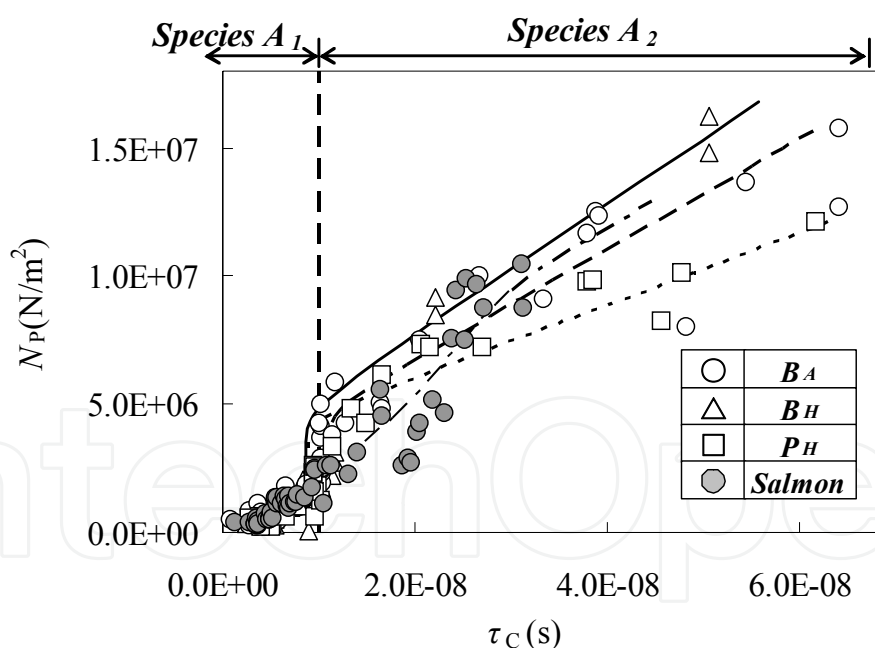

Fig. 20. Comparing behavior of N_P as a function of τ_C between B_A, B_H, and P_H at 50°C.

6.4 Physical meaning of $C\tau_C = 10^{-8}$ s derived from the pre-exponential factor (De^0) of De

Focusing on the boundary ($C\tau_C = 10^{-8}$ s) between water species A_1 and A_2, one may be interested in what is happening in the food tissue matrix at the $C\tau_C = 10^{-8}$ s. The information for the food tissue matrix can be obtained from Equation (2), and the equation is rewritten by Equation (10). The pre-exponential factor (δD_0) of Equation (10) consists of a function of ε,

χ, and ΔS. Since the δD_0 value can be evaluated from the extrapolation of the Arrhenius plots against the perpendicular axes in Fig. 13, those evaluated for B_A, B_H, and P_H can be plotted as a function of τ_C, as shown in Figure 21. Three δD_0 curves obtained demonstrate a steep decay at the $C\tau_C = 10^{-8}$ s. Based on the rough evaluation of the steep decay for the three curves to be 1/30 ~1/150, the reduction of the δD_0 values should be attributed to a simultaneous change in the ε value, which becomes smaller while the χ value becomes larger and the ΔS value becomes smaller because of the steep change in the physical structure of the B_A, B_H, and P_H's tissue matrix at the $C\tau_C = 10^{-8}$ s derived from dehydration.

$$De = \delta D_0 \cdot exp\left(\frac{-E_D}{R \cdot (T_D + 273)}\right) = \left(\frac{\varepsilon}{\chi}\right) \cdot \left(\frac{k \cdot (T_D + 273)}{h}\right)\left[exp\left(\frac{\Delta S}{R}\right)\right] \cdot exp\left(\frac{-E_D}{R \cdot (T_D + 273)}\right)$$ (10)

where k is Boltzmann constant, h is Planck constant, $\delta(=\varepsilon/\chi)$ is diffusibility, ε is porosity, χ is labyrinth factor, and ΔS is activation entropy.
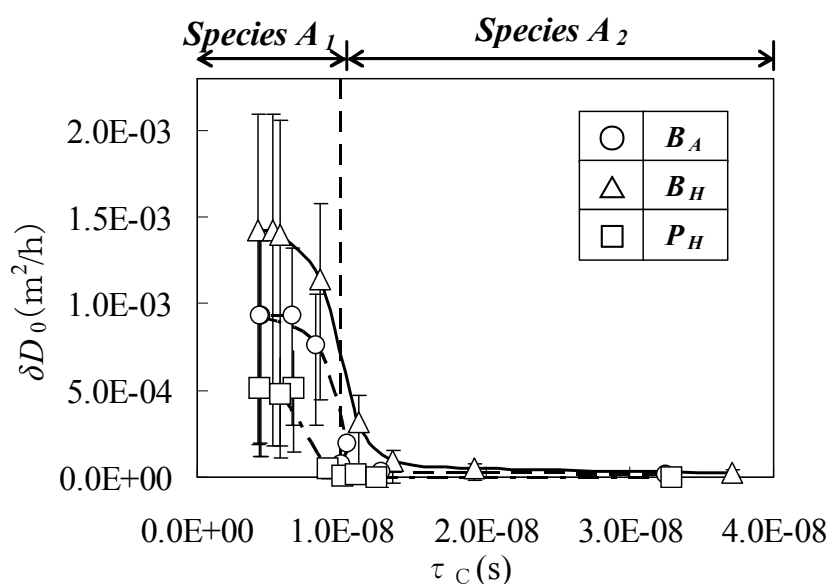

Fig. 21. Comparing behavior of the pre-exponential factor between B_A, B_H, and P_H at 50°C as a function of τ_C.

Figure 22 illustrates the optical microscope photographs of the cross-section for B_H. Comparing Figs. 22(A) and (B), one can clearly recognize that a large number of pores (complicated structures) appeared in the sample of $W_0 = 54\%$-d.b. rather than that of $W_0 = 127\%$-d.b., indicating a growth of the labyrinth factor (χ). This growth of χ contributes to the reduction of δ and is supported by the experimental evidences of the steep reductions of both δD_0 in Fig. 21 and De in Fig. 19 in the water species A_2 region.

The $\delta D_0 \sim \tau_C$ plots again demonstrate the hybrid technique to be a useful tool for discriminating between the two water species and among the kind of foods. The drastic change of δD_0 should derive the change of water species from A_1 to A_2, suggesting the diffusion mechanism change between the two regions. This idea is strongly supported by experimental evidence as shown in Figure 23. All E_D's of water species A_2 for B_A, B_H, and P_H demonstrated a drastic reduction at $C\tau_C$ in the water species A_2 region. This reduction of E_D strongly suggests a change in the diffusion mechanism from the water species A_1 region.

Fig. 22. Optical microscope photographs (× 1000) of the cross-section for P_H, (A): 127%-d.b., (b): 54%-d.b.
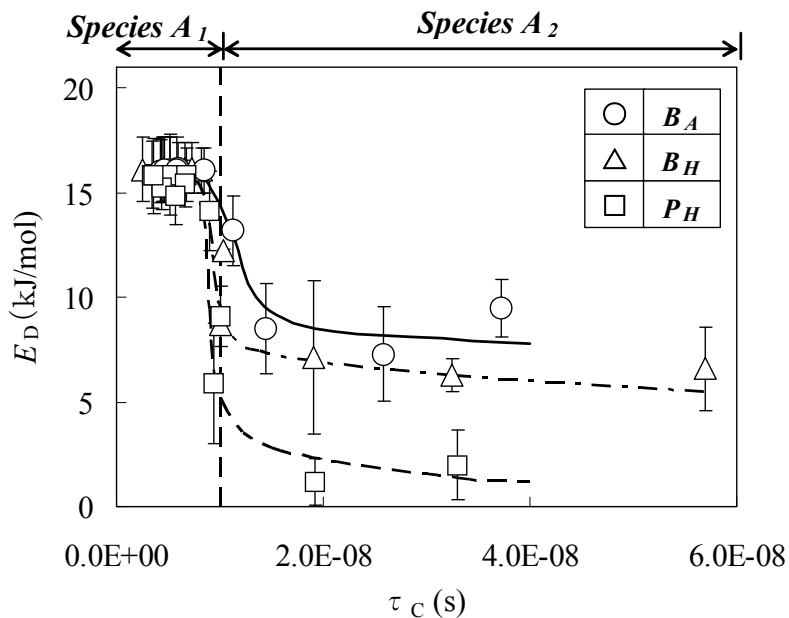

Fig. 23. Comparing behavior of E_D among B_A, B_H, and P_H as a function of τ_C at 50~70°C.

7. A new method for jerky product design using the parameters induced by the hybrid technique

Our interest is focused on a classification of the 12 jerky products influenced by multifunctional water species. Hills *et al.* (1999) empirically demonstrated a linear relation between the NMR relaxation rates ($1/T_2$) and a_w. In addition, Hills (1999) derived a theoretical equation to explain the linear relation. Since the relaxation time, T_2, can be replaced by τ_C using Equation (3), it is proposed that a_w should be related to τ_C. Figure 24 demonstrates a_w as a function of τ_C for the 12 jerky samples. All the samples fell roughly around three straight lines, indicating the existing of three groups. The three lines started from $a_w = 0.92$, which is an identical value independent of the samples and empirically evaluated, meaning a specified value for all kinds of foods (Konishi and Kobayashi, 2010). The $a_w = 0.92$ value always gave $\tau_C = 10^{-8}$ s independent of the kinds of foods and seasoning species. As has been discussed in the previous section, one can recognize both $a_w = 0.92$ and $\tau_C = 10^{-8}$ s to be critical values for foods in which the water species drastically changes from

A_1 to A_2 and the pore structure of the food tissue matrix provides regulation of ε and χ values accompanied by drastic increases or decreases.

Focusing on the three straight lines in Fig. 24, line-1 generates Group-1 (BJ-5 and PJ-2), line-2, Group-2 (BJ-4, BJ-1, PJ-4, BJ-6, and PJ-1), and line-3, Group-3 (PJ-5, BJ-3, BJ-2, and PJ-6). Based on the experimental data presented here, although one cannot demonstrate an exact physical meaning of the three groups' difference, it might be presumed that each group should have the specified seasonings different from others. Concerning the seasonings in the three groups, Group-1 is characterized by soy sauce, Group-2, by a mixed seasoning such as soy sauce, smoke flavoring, and salt, and Group-3, by a mixed seasoning such as salt, soy-sauce, and miso sauce. Although each of the three groups could not be distinguished by the chemical engineering (the aw ~ W_0 curves and the De ~ W_0 curves) and proton NMR techniques (the τ_C ~ W_0 curves), the hybrid technique (the aw ~ τ_C linear relation) clearly distinguished the characteristics of the seasonings for the 12 different food products. This evidence strongly demonstrates the hybrid technique to be a useful tool to design various food products requested by the commercial fields.
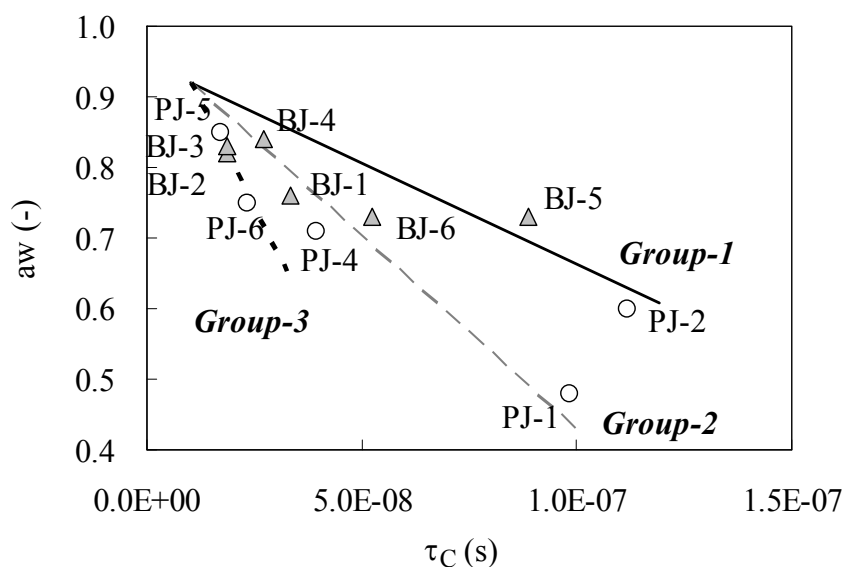

Fig. 24. a_w as a function of τ_C for the beef and pork jerkies.

8. Conclusions

The hybrid of the proton NMR technique and the chemical engineering technique was applied to discriminate the 12 commercially distributed jerkies, salmon, B_A, B_H, and P_H and to distinguish between the two water species, A_1 and A_2, by using four parameters: De, τ_C, N_P, and W_0 .

1. The dehydration and adsorption of the water species, A_1 and A_2, retained in the foods were reversibly repeated and the transformation between the two water species was reproducible.
2. The proton NMR technique and the chemical engineering technique could respectively not discriminate among the τ_C ~ W_0 curves and among the a_w ~ W_0 curves obtained for the foods. Although the computer simulation model proposed by the chemical engineering technique generated a good fitting against the dehydration response

curves, the unknown parameters evaluated by the curve fitting, β_1 and β_2, were recognized as meaningless.

3. The hybrid technique proposed demonstrates a clear discrimination between water species A_1 and A_2, divided at the critical value of $C\tau_C = 10^{-8}$ s, where the drastic change in the values of De, E_D, and N_P appeared. The physical meaning of $C\tau_C$ was understood as a drastic change in the pre-exponential factor of De derived from the change in the food tissue matrix due to dehydration.

4. Using the hybrid technique, a variety of food products could easily be designed by changing the value of τ_C even though the values of a_w are identical. The meat jerkies commercially distributed in Japan were reasonably classified into three groups characterized by the three $a_w \sim \tau_C$ straight lines. The advantage of the hybrid technique brought a conclusion that the $a_w \sim \tau_C$ straight lines give characteristic slopes depending on the seasonings of the 12 jerkies. This could be useful in designing a variety of food products.

9. Nomenclature

B_A	*beef meat produced in Australia* (-)
B_H	*beef meat produced in Hokkaido, Japan* (-)
D	*moisture diffusion coefficient* (m²/h)
D_0	*frequency factor of D* (m²/h)
De	*effective water diffusion coefficient* (m²/h)
De^0	*pre-exponential factor of De* (PF=δ·D_0 , m²/h)
E_D	*activation energy of water diffusivity* (kJ/mol)
H	*Planck constant* (erg. s)
I	*nuclear spin quantum number of water proton* (= 0.5) (--)
K	*Boltzmann constant* (erg/deg)
k_S	*mass transfer coefficient of strongly restricted water* (h⁻¹)
k_w	*mass transfer coefficient of weakly restricted water* (h⁻¹)
L_a	*half distance of a-axis of the rectangular sample* (m)
L_b	*half distance of b-axis of the rectangular sample* (m)
L_c	*half distance of c-axis of the rectangular sample* (m)
M_t	*magnitude of magnetization vector* (-)
M_0	*magnitude of macroscopic equilibrium magnetisation vector* (-)
N_P	*hardness of meat products* (Newton/m²)
P_H	*pork meat produced in Hokkaido, Japan* (-)
R	*gas constant* (=8.314J/K mol)
r	*proton-proton distance of water molecule* (= 0.16 nm)
ΔS	*activation entropy* (kJ/mol)
T_2	*spin-spin relaxation time of water proton* (s)
T_D	*drying temperature* (°C)
t	*drying time* (h)
ts	*spin locking pulse length* (s)
W	*water content at the drying time t* (%-d.b.)
W_0	*initial water content at the time of PUP operated* (%-d.b.)
W_D	*initial water content of drying flesh sample* (%-d.b.)
We	*equilibrium water content* (%-d.b.)

W_R	*the water ratio (= (W-We)/(W$_D$-We))*
W_{R1}	*the proportion of the strongly restricted water amount (-)*
W_{R2}	*the proportion of the weakly restricted water amount (-)*
W_{RS}	*the ratio of the strongly restricted water species (-)*
W_{RW}	*the ratio of the weakly restricted water species (-)*
W_S	*the amount of strongly restricted water species (%-d.b.)*
W_W	*the amount of weakly restricted water species (%-d.b.)*

Greek letters

| β_1	*constant evaluated by the curve fitting simulation (m^{-2})*
β_2	*constant evaluated by the curve fitting simulation (m^{-2})*
ε	*porosity of the food tissue (-)*
π	*the ratio of the circumference of a circle to its diameter (=3.14)*
γ	*gyromagnetic ratio of proton (=2.675×10^8 rad·T^{-1}·s^{-1})*
$\hbar$	*modified Plank's constant (=6.63×10^{-34} J·s)*
ω_0	*resonance frequency (=3.14×10^9 s^{-1})*
τ_C	*correlation time of water proton (s)*
$C\tau_C$	*critical correlation time of water proton (s)*
χ	*labyrinth factor of the meat tissue (-)*
δ	*diffusibility (=ε /χ)(-)*

10. Acknowledgment

11. References

Abragam, A., (1963). The Principles of Nuclear Magnetism. *Oxford at the Clarend Press*, p347-349.

Andreu, J. & Stamatopoulos, A.A. (1986). Durum wheat pasta drying kinetics. *Lebensm. Wiss. u.-Technol.*, 19 , 448-456.

Belton, P.S.; Gil, A.M.; Webb, G.A., & Rutledge, D., Eds.(2003). Magnetic resonance in food science-latest developments, *The Royal Society of Chemistry, Cambridge*.

Chhinnan, M.S. (1984). Evaluation of selected mathematical models for describing thin-layer drying of in-shell pecans. *Trans. ASAE*, 27(2), 610-615.

Fennema, O.(1976). In principles of food science, Part 1, Marcel Dekker, New York.

Hills, B.P. (1999). NMR studies of water mobility in foods. In"Water Management in the Design and Distribution of Quality Foods" ISOPOW 7(Y.H. Roos, R.B. Leslie, and P.J.Lillford, eds) Technomic Publishing, Lancaster, PA.

Hills, B. P., Manning, C. E. & Godward, J. (1999). A multistate theory of water relations in biopolymer systems. In: *Advances in Magnetic Resonance in Food Science* (edited by P. S. Belton, B. P. Hill and G. A. Webb). Pp.45-62. Cambridge, UK: Royal Society of Chemistry.

Jason, A.C.(1958). A Study of evaporation and diffusion processes in the drying of fish muscle in fundamental aspects of dehydration of food stuffs, ed. Society of Chemical Industry. *McMillan, London*, pp.103-134.

Kannan, D. and Bandyopadhyay, S. (1995). Drying characteristics of a tropical marine fish slab. *J.Food Sci. Technol.*, 32(1), 13-16.

Konishi, Y.; Horiuchi, J., & Kobayashi, M.(2001). Dynamic evaluation of the dehydration response curves of foods characterized by a poultice-up process using a fish-paste sausage-I. Determination of the mechanisms for moisture transfer, *Drying Technology*, 19(7), 1253-1269

Konishi, Y.; Horiuchi, J., & Kobayashi, M.(2001). Dynamic evaluation of the dehydration response curves of foods characterized by a poultice-up process using a fish-paste sausage-II, A new tank model for a computer simulation, *Drying Technology*, 19(7), 1271-1285.

Konishi, Y.;Miura, K. & Kobayashi, M.(2003). Drying efficiency design using multifunctional dynamics of water molecules in foods-H-NMR analysis of a fish paste sausage and squid, *AIDIC Conference series,* vol.6, 183-190.

Konishi, Y. & Kobayashi, M.(2009). Quantitative evaluation of the design parameters requested in beef and pork drying operation, *AIDIC Conference Series*, 9, 177-186.

Konishi, Y., & Kobayashi, M., (2010). Food product design using the water species as a probe molecule. Annual meeting of Japanese Society of Food Engineering.

Konishi, Y., Kobayashi, M., & Miura, K. (2010). Characeterization of water species revealed in the drying operation of Todarodes pacificus Steenstrup using water proton NMR analysis, *International Journal of Food Science and Technology.*, 45.1889-1894.

Konishi, Y. & Kobayashi, M.(2011). Dynamism of the water species as a probe molecule in food, *Chemical Engineering Transactions*, Ed. Sauro Pierucci, 24, 475-480.

Labuza, T.P., Tannenbaum, S.R., & Karel,M. (1970), Water Content and Stability of Low moisture and intermediate moisture foods. Food Technol.24, 543-550.

Litchfield, J.B. & Okos, M.R. ,1992. Moisture diffusivity in pasta during drying. *J. Food Engng.*, 17, 117-142.

Madamba, P. S., Driscoll, R. H. & Buckle, K. A.(1996). The thin-layer drying characteristics of garlic slices. *J. Food Engng.*, 29, 75-97.

Noomhorm, A. & Verma, L.R.(1986). Generalized single layer rice drying models. *Trans. ASAE.*, 29(2), 587-591.

Rockland, L.B. and Stewart, G.F., Eds.(1981). International symposium on properties of water, water activity: Influences on food quality, *Academic Press Inc., London.*

Schmidt, S.J., Water and Solids Mobility in Foods, (2004). Advances in Food and Nutrition research, volume 48, 2004, Edited by S.L. Taylor, Elsevier

Thompson, T.L., Peart, R.M. & Foster, G.H. (1968). Mathematical simulation of corn drying (A new model). *Trans.ASAE.*,24(3),582.

Waananen, K.M. & Okos, M.R. (1996). Effect of porosity on moisture diffusion during drying of pasta. *J. Food Engng.*, 28, 121-137.
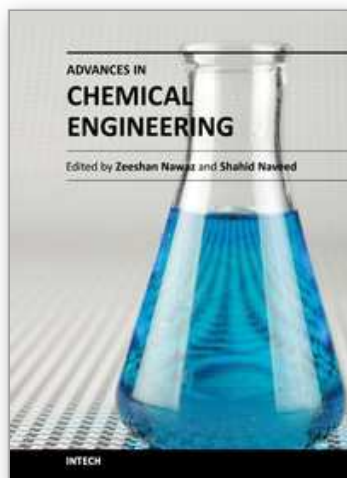
Advances in Chemical Engineering

Edited by Dr Zeeshan Nawaz

Chemical engineering applications have been a source of challenging optimization problems in terms of economics and technology. The goal of this book is to enable the reader to get instant information on fundamentals and advancements in chemical engineering. This book addresses ongoing evolutions of chemical engineering and provides overview to the sate of the art advancements. Molecular perspective is increasingly important in the refinement of kinetic and thermodynamic molding. As a result, much of the material was revised on industrial problems and their sophisticated solutions from known scientists around the world. These issues were divided in to two sections, fundamental advances and catalysis and reaction engineering. A distinct feature of this text continues to be the emphasis on molecular chemistry, reaction engineering and modeling to achieve rational and robust industrial design. Our perspective is that this background must be made available to undergraduate, graduate and professionals in an integrated manner.

How to reference

In order to correctly reference this scholarly work, feel free to copy and paste the following:

Yasuyuki Konishi and Masayoshi Kobayashi (2012). Challenging Evaluation of the Hybrid Technique of Chemical Engineering - Proton NMR Technique for Food Engineering, Advances in Chemical Engineering, Dr Zeeshan Nawaz (Ed.), ISBN: 978-953-51-0392-9, InTech, Available from: http://www.intechopen.com/books/advances-in-chemical-engineering/challenging-evaluation-of-a-hybrid-method-of-chemical-engineering-proton-nmr-technique-for-the-food-

INTECH
open science | open minds